

# Direct determination of the spiral pattern rotation speed of the Galaxy

Wilton S. Dias<sup>1</sup>  
 and  
 J.R.D.Lépine<sup>2</sup>

## ABSTRACT

The rotation velocity of the spiral pattern of the Galaxy is determined by direct observation of the birthplaces of open clusters of stars in the galactic disk as a function of their age. Our measurement does not depend on any specific model of the spiral structure, like the existence of a given number of spiral arms, or the presence of a bar in the central regions. This study became possible due to the recent completion of a large database on open clusters by our group. The birthplaces of the clusters are determined by two methods, one that assumes that the orbits are circular, and the other by integrating the orbits in the Galactic potential for a time equal to the age of the clusters. We selected in the database a sample of 212 clusters for which proper motions, radial velocities, distances and ages are available, or of 612 clusters that have ages and distances available. We tested different assumptions concerning the rotation curve and the radius  $R_0$  of the solar orbit. Our results confirm that a dominant fraction of the open clusters are formed in spiral arms, and that the spiral arms rotate like a rigid body, as predicted by the classical theory of spiral waves. We find that the corotation radius  $R_c$  is close to the solar galactic orbit ( $R_c/R_0 = 1.08 \pm 0.08$ ). This proximity has many potentially interesting consequences, like a better preservation of life on the Earth, and a new understanding of the history of star formation in the solar neighborhood, and of the evolution of the abundance of elements in the galactic disk.

*Subject headings:* Galaxy: spiral arms: Galaxy - corotation

## 1. Introduction

According to the classical theory of galactic spiral waves proposed by Lin & Shu (1964) and Lin et al. (1969), the spiral arms are restricted to the interval between the inner and outer Lindblad resonances (ILR and OLR), where the pattern angular velocity  $\Omega_p$  equals  $\Omega \mp \kappa/2$ , where  $\Omega$  is the angular rotation velocity of the disk and  $\kappa$  is the epicycle frequency. The spiral pattern is considered to rotate like a rigid disk, while the gas and stars present differential rotation. The radius

where  $\Omega = \Omega_p$ , called corotation radius, is situated between the ILR and the OLR. Since  $\kappa$  is a function of  $\Omega$  and of its derivative  $d\Omega/dr$  only (eg. Binney and Tremaine, 1987), given the rotation curve of the Galaxy, the position of the Lindblad resonances depend only on the pattern rotation speed.

The radii of those resonances and of corotation in our Galaxy have been a subject of controversy. Lin and his collaborators situated the corotation at the edge of the galactic disk, at about 16 kpc from the center. Other authors like Amaral & Lépine (1997) and Mishurov & Zenina (1999) claimed that the corotation is close to the radius of the solar orbit  $R_0$ . This view is supported by recent studies of metallicity gradients in the galactic disk (Andrievski et al, 2004, Mishurov et al., 2002). Yet another group of researchers be-

<sup>1</sup>Instituto de Física de São Carlos, Universidade de São Paulo, Caixa Postal 369, São Carlos 13560-970, SP, Brazil

<sup>2</sup>Instituto de Astronomia, Geofísica e Ciências Atmosféricas, Universidade de São Paulo, Cidade Universitária, São Paulo, SP, Brazil; E-mail: jacques@iagusp.usp.br

lieves that the spiral pattern rotates so fast that the corotation resonance is situated in the inner part of the Galaxy at  $r \approx 3 - 4 \text{ kpc}$  and the OLR is located close to the Sun (e.g. Weinberg 1994; Englmaier & Gerhard 1999; Dehnen 2000, etc.). In parallel with the quasi-stationary models just mentioned, there are quite different interpretations of the spiral structure, like those of Binney & Lacey (1988) and of Sellwood & Binney (2002), who consider that the arms are constituted by a series of transient waves with different pattern velocities (and consequently, different corotation radii), and that of Seiden & Gerola (1979), who argue that the arms are not density waves but the result of a stochastic self-propagating star formation process.

It is therefore an important step in the understanding of the spiral structure to firmly establish what is the rotation velocity of the spiral pattern in the Galaxy, as well as to verify if different arms have the same velocity. In the present paper we present a new method to measure the velocity of the spiral arms, based on the orbits of a sample of open clusters, which have known distances, space velocities and ages.

## 2. The Open Clusters Catalog

We make use of the *New Catalogue of Optically visible Open Clusters and Candidates* published by Dias et al. (2002) and updated by Dias et al. (2003)<sup>3</sup>. This catalog updates the previous catalogs of Lyngå (1987) and of Mermilliod (1995). The present version of the catalog contains 1689 objects, of which 599 (35.5%) have published distances and ages, 612 (36.2%) have published proper motions (most of them determined by our group, Dias et al., 2001, 2003) and 234 (13.8%) have radial velocities.

## 3. Basic assumptions

The basic assumption is that star formation, and in particular, open cluster formation, takes place only (or almost only) in spiral arms. This follows from the ideas of Roberts (1969), Shu et al. (1972), and many others, according to whom the shock waves occurring in spiral arms are the

triggering mechanism of star formation. There is observational evidence that this is true in external spiral galaxies, where we see the HII regions and massive stars concentrated in spiral arms. The fact that young open clusters are tracers of the spiral structure has been known for several decades (eg. Becker & Fenkart, 1970). The distribution of open clusters in the Galactic disk is shown in Figure 1, for clusters younger than 7 Myr, and in Figure 2, for clusters older than 30 Myr. It is clear that in about 20 Myr the open clusters drift away from the arms and fill the inter-arm regions. It will be shown in this work that the structure that has disappeared in Figure 2 can be retrieved by a proper correction of the cluster positions.

After their birth, the clusters follow Galactic orbits that can be easily calculated, since we know the galactic potential. Knowing the present day space velocity components, we can integrate each orbit backwards for a time interval equal to the age of the cluster, and find where the clusters were born. The birthplace of each cluster indicates the position of a spiral arm at a past time equal to its age. In principle, it is not difficult to trace the motion of the arms. Our task is to find the most reliable way to extract this piece of information from the clusters data.

Before looking for precise methods to determine the corotation radius, we call attention to the fact that a direct inspection of the distribution of the clusters in the galactic plane, gives an approximate value of that radius, in a way that does not depend on any particular choice of a rotation curve or of a set of galactic parameters. Let us compare Figure 1 with Figure 3; the difference between the two figures is the range of age of the clusters. The lines representing the position of the arms in Figure 1 (age  $< 7 \text{ Myr}$ ) are reproduced as guidelines in Figure 3 (12 Myr  $<$  age  $<$  25 Myr). These lines represent approximately the present day position of the arms. In Figure 3, most of the clusters associated with the Perseus arm (the outer arm in the figure) are situated to the left of the line. In contrast, most of the clusters associated with the Sagittarius-Carina arm (the inner arm in the figure) are situated to the right of the corresponding line. This means that the clusters that were born some 10-20 Myr ago, and since then are rotating around the galactic center with about the velocity of the rotation curve, have rotated slower than the

<sup>3</sup>Available at the web page <http://astro.iag.usp.br/~wilson>

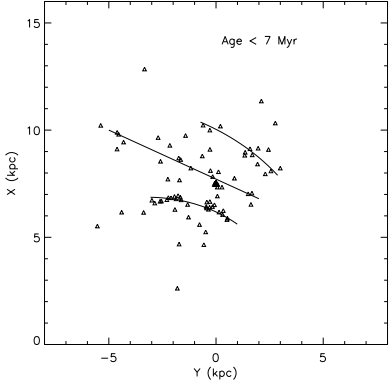


Fig. 1.— The sample of open clusters with age < 7 Myr in the solar neighborhood. The Sun is at coordinates (0, 7.5); the Galactic center at (0,0); distances are in kpc.

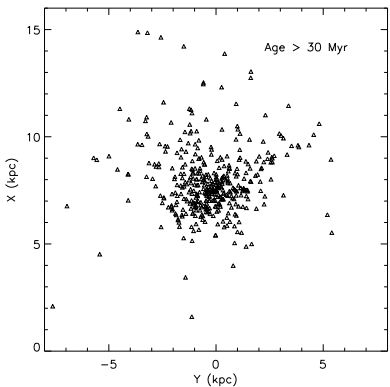


Fig. 2.— The sample of open clusters with age > 30 Myr in the solar neighborhood.

spiral pattern at the outer radii, and faster than the spiral pattern at the inner radii. This is what we expect to observe, if the corotation radius is between the two arms, that is, close to the Sun.

### 3.1. Methods to determine the pattern speed

We propose two methods to trace back the orbits of the clusters and find their birthplace, that we shall call "true integration" and "circular rotation", and two methods to derive the rotation velocity of the arms, based on the birthplaces of the clusters; we shall call them "direct observation of pattern rotation" and "reconstruction of the present day arms". We present in this work the best two combinations of these methods. We next explain the reasons for the use of different methods to retrieve the birthplaces.

In principle, by performing a true integration of the orbit, using the observed space velocities as initial conditions, one takes into account the fact that the orbits are not precisely circular, and one obtains the best birthplace determinations. However, true integration is limited to the sample of clusters which have, in the catalog, distance, age, proper motion and radial velocity. At the moment, this amounts to a total of 212 objects only. When we further restrict the sample to some narrow ranges of ages, as required by one of the methods discussed below, the available number of clusters becomes too small. Furthermore, one must remember the components of the space velocities given in the catalog, in particular the radial velocities, are affected by errors, so that the initial conditions of the orbit integrations have uncertainties. These reasons led us to use simple circular rotation as an alternative method. In this case, the orbits of the clusters are supposed to be circular. The birthplaces are found by assuming that the clusters moved a distance equal to their age multiplied by their velocity, given by the rotation curve. Therefore, the only parameters needed to recover the birthplaces are distances and ages; in this case the available sample in our database amounts to 599 objects.

### 3.1.1. Direct observation of pattern rotation (Method 1)

The simplest way to proceed, once the birthplaces of the clusters have been obtained, is to directly observe the rotation of the pattern that they form, as illustrated in Figure 4. We first fitted segments of spirals (indicated by dashed lines) to the birthplaces of a sample of very young clusters (5-8 Myr, not shown). The adopted equation of spiral arms is  $r = r_i \exp(k\theta + \phi_0)$ , where  $r_i$  is the initial radius,  $\phi_0$  the initial phase angle and  $k = \tan(i)$  is a constant related to the inclination  $i$  of the arm. We then rotate those spiral segments around the Galactic center by varying  $\phi_0$ , so as to obtain the best fit of an older sample (9-15 Myr, clusters birthplaces shown as squares, fitted solid lines); the rotation angle in this example is  $\alpha = 10^\circ$ . We emphasize that Figure 4 is different from Figure 3 and previous ones, in the sense that we are plotting the birthplaces, not the present day position of the clusters. It is important to remark that a same rotation angle fits correctly the different arms, based on our sample of clusters.

The variation of the rotation angle with the age of the samples is shown in Figure 5. The successive age ranges that were used are indicated in the caption. For each age range, the only parameter used to fit the pattern is the angle  $\alpha$ , like in Figure 4. In order to maximize the number of clusters in each sample, we allowed a small overlap of the age ranges, and we adopted the birthplaces obtained by circular rotation of the clusters, as already explained.

The procedure to find the best fit parameter  $\alpha$  for each age range was the following. For each of the 3 arms, we selected as belonging to the arm the clusters that are at a distance smaller than 0.5 kpc from it. For these clusters, we computed the sum of the components of the distances to the arm, in the Y direction (defined here as the horizontal direction in the figure, which is about the direction of rotation of the Galaxy, for objects close to the Sun). When this sum is zero, this means that there are about the same number of clusters to the right and to the left of the arm, which gives the best fit.

The birthplaces depend obviously on the adopted rotation curve. As later discussed, we tested different rotation curves and values of  $R_0$ . In Figure 5 we compare the results for two flat rotation

curves, with  $V_0 = 170 \text{ km s}^{-1}$  and  $V_0 = 190 \text{ km s}^{-1}$ , for  $R_0 = 7.5 \text{ kpc}$ . The slopes of the fitted lines are respectively  $1.16^\circ/\text{Myr}$  and  $1.33^\circ/\text{Myr}$ . It is an expected result that when we adopt a larger rotation velocity, the birthplaces are found more distant from the solar neighborhood, and a larger rotation velocity of the pattern is derived. Note that  $1^\circ/\text{Myr}$  is equivalent to  $17 \text{ km s}^{-1} \text{kpc}^{-1}$ , the derived corotation radii ( $= V_0/\Omega_p$ ) are 8.6 and 8.1 kpc respectively in this example

### 3.1.2. Reconstruction of spiral arms (Method 2)

Although it is usually accepted that young galactic objects have near-circular orbits, it is important to check if the hypothesis of circular motion can be responsible for systematic errors in the determination of the pattern rotation speed. For instance, it is expected that the shock waves in the spiral perturbation potential produces a braking the molecular clouds (and consequently, of the recently formed stars) at galactic radii smaller than the corotation radius, and an acceleration of the molecular clouds at larger radii. It is therefore necessary to perform experiments with exact integration of the orbits, in order to take into account the initial velocity perturbation.

The method previously described to derive the pattern rotation velocity requires a sufficiently large number of clusters in each age bin. The second method that we propose here does not separate the clusters into age bins, and makes use of a sample with a wide range of age. This is convenient to work with the small sample of clusters for which it is possible to perform exact integration of the orbits.

In this method, as a first step, we find the birthplace of each cluster, integrating backwards their orbits for time intervals  $T$  equal to their age, starting from the present day initial conditions (positions and space velocities). The method of integration is discussed later. The birthplace of a cluster is supposed to represent a point of a spiral arm, a time  $T$  ago. If we rotate forward this point an angle  $\Omega_p * T$  around the galactic center, we obtain a point situated on the present day position of the arm. In this way, points corresponding to very different ages can be used to trace the present day arms. The unknown is  $\Omega_p$ . The best estimate of  $\Omega_p$  is the one that gathers the maximum number of points close to the present day position

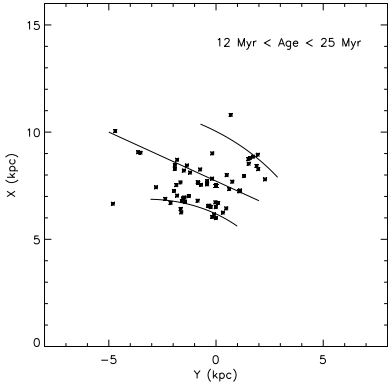


Fig. 3.— The sample of open clusters with  $12 \text{ Myr} < \text{age} < 25 \text{ Myr}$  in the solar neighbourhood. Actual positions are plotted.

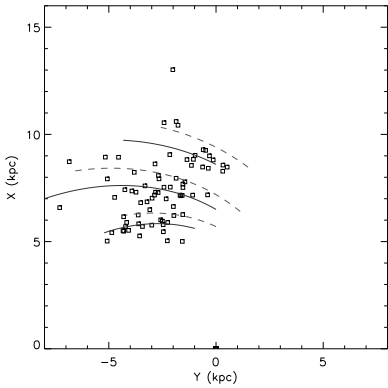


Fig. 4.— Birthplaces of the clusters with ages in the range 9-15 Myr (average 11.6 Myr), in the galactic plane. The dashed lines were fitted to a younger sample, not shown, with ages in the range 5-8 Myr (average 6.3 Myr); the solid lines are the same arms of the dashed line, rotated by  $10^\circ$  around the galactic center. This angle is the best fit to the sample displayed.

of the arms. In practice, the best value of  $\Omega_p$  is found in an interactive mode, using a technique similar to that of the previous method. We select the points that are within 0.5 kpc of any of the 3 arms (to avoid mixing of arms), and we minimize the rms distance to the arms, varying  $\Omega_p$ . However, we do not know a priori the present day position of the arms, because there are almost no cluster younger than 5 Myr. Even if we selected a young sample, we would need to correct the observed positions, using  $\Omega_p$ . Therefore, we use an interactive method: for each adopted  $\Omega_p$ , we allow minor variations in the parameters describing the arms, in order to minimize the rms distance of the points to them. Next we compare the rms distances obtained with different values of  $\Omega_p$ . We illustrate in Figure 6 the results obtained with this method, using a CO-based rotation curve (see below). The adjusted points were from the sample of clusters in the range 10-30 Myr. The same result is obtained if we use another range, like 10-50 Myr. However, the absolute errors on the age tend to increase with the age, and it is preferable not to exceed 30 Myr. The derived value of  $\Omega_p$  is  $25 \pm 1 \text{ km s}^{-1} \text{kpc}^{-1}$ , which correspond to a corotation radius of  $7.6 \pm 0.3 \text{ kpc}$ , for  $R_0 = 7.5 \text{ kpc}$  and  $V_0 = 190 \text{ km s}^{-1}$ .

### 3.1.3. Rotation curves and details of orbit integration

Most of the open clusters in the catalog of Dias et al. are situated at galactic radii in the range  $R_0 \pm 2 \text{ kpc}$ , so that our calculations only make use the portion of the rotation curve situated in this range. Since the rotation curve of the Galaxy is known to be relatively flat close to the Sun, a linear approximation of it is sufficient, in this interval. The only important parameters are the rotation velocity of the LSR,  $V_0$ , and the slope of the rotation curve,  $(dV/dR)_{R_0}$ . These parameters are linked together and with the value of  $R_0$  through the Oort's constants  $A$  and  $B$ , which are determined by observations ( $V_0/R_0 = A - B$ ,  $(dV/dR)_{R_0} = -A - B$ ). The  $R_0$  value 8.5 kpc, recommended by the International Astronomical Union, is often used in the literature with  $V_0 = 220 \text{ km s}^{-1}$ , which corresponds to  $A - B = 26 \text{ km s}^{-1} \text{kpc}^{-1}$  (eg. Binney & Tremaine, 1987). This value of  $A - B$  seems to be well established, and is confirmed by recent observations of a different na-

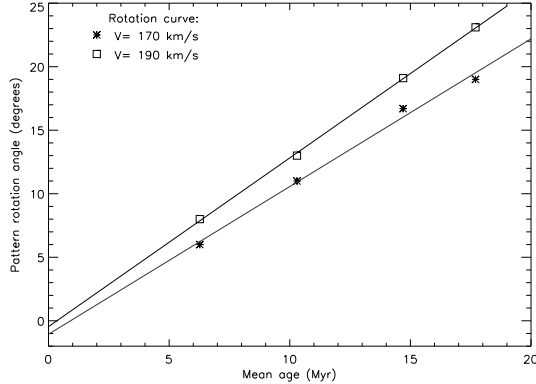


Fig. 5.— Rotation angle required to fit the birth-places of samples of clusters of different ages with a spiral pattern that represents the present day structure (Method 1). In this example, the birth-places were determined with two flat (constant velocity) rotation curves, with  $V_0 = 170 \text{ km s}^{-1}$  and  $V_0 = 190 \text{ km s}^{-1}$ . The age range of the samples, in Myr, were 0-8 (average 6.27), 7-14 (average 10.3), 12-18 (average 14.7), 15-22 (average 17.7)

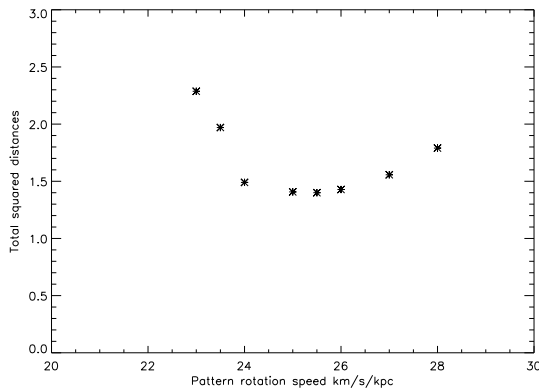


Fig. 6.— Procedure to find the best estimate of pattern rotation velocity  $\Omega_p$  (Method 2). The best value ( $25 \text{ km s}^{-1} \text{kpc}^{-1}$ ) is given by the minimum for sum of the squared distances from the points to the fitted arms. This example corresponds to  $R_0 = 7.5 \text{ kpc}$  and  $V_0 = 190 \text{ km s}^{-1}$ .

ture (Kalirai et al., 2004) which give  $25.3 \pm 2.6 \text{ km s}^{-1} \text{kpc}^{-1}$ . Recent works often adopts  $R_0 = 7.5 \text{ kpc}$  (Racine & Harris, 1989, Reid, 1993, and many others). The shorter scale is supported by VLBI observations of  $\text{H}_2\text{O}$  masers associated with the Galactic center. Keeping the same value for A-B, the corresponding  $V_0$  would be  $195 \text{ km s}^{-1}$ . We note that Olling & Dehnen (2003) argue that the rotation curve is flat ( $A = -B$ ), but usually, the rotation curve is considered to be decreasing near the Sun, with  $-A-B$  about  $-3 \text{ km s}^{-1} \text{kpc}^{-1}$  (Binney & Tremaine, 1987).

We calculated  $\Omega_p$  for two values of  $R_0$ , 7.5 and 8.5 kpc, each combined with different values of  $V_0$  (170, 190 and 210  $\text{km s}^{-1}$  for  $R_0 = 7.5 \text{ kpc}$ , and 180, 200 and 220  $\text{km s}^{-1}$  for  $R_0 = 8.5 \text{ kpc}$ ), considering both flat curves and curves similar to that of Clemens (1985). The original curve obtained by Clemens assumed  $R_0 = 8.5 \text{ kpc}$  and  $V_0 = 220 \text{ km s}^{-1}$ . We used the same observational CO data of Clemens to reconstruct the curve for different values of  $R_0$  and  $V_0$ . In each case we fitted the curve with a simple analytical expression, in order to use it in the calculations. An example of these CO-based curves, for  $R_0 = 7.5 \text{ kpc}$  and  $V_0 = 190 \text{ km s}^{-1}$ , is shown in Figure 7. The fitted curve has a linear behavior close to the Sun, with a slope about  $-3.3 \text{ km s}^{-1} \text{kpc}^{-1}$ . For this curve in particular, both  $V_0/R_0$  and  $(dV/dR)_R$  are in agreement with the best estimate of Oort's constants.

To perform numerical integration of the orbits, the observed radial velocities and proper motions were corrected for differential rotation before being converted to U, V, W velocities in the galactic local system. The corrections in radial velocity, and proper motions in longitude and latitude directions ( $\mu_l \cos(b)$  and  $\mu_b$ ) are respectively (eg Carraro & Chiosi, 1994):  $C_{rv} = A \cos(2l) \sin(2b)$  ;  $C_{pmi} = (A \cos(2l) + B) \cos(b) / 4.74$  ;  $C_{pmb} = A \sin(2l) \sin(2b) / 24.74$ , where  $l, b$  are the galactic coordinates,  $d$  the distance,  $A, B$  the Oort's constants. For each galactic rotation curve that we used, we first made the proper motion correction using the corresponding values of  $A$  and  $B$ . Another correction is the transformation of the velocities to the Local Standard of Rest; we assumed that the Sun has a velocity  $22 \text{ km s}^{-1}$  in the direction  $l = 61.4^\circ, b = 20.4^\circ$  (Abad et al., 2003).

#### 4. Results and conclusions

The galactic corotation radii  $R_c$  derived in this work are summarized in Table 1. Typical errors on individual determinations are about  $\pm 0.3$  kpc. The values of  $R_c$  that we obtain with different methods and different sub-samples of open clusters are quite consistent.  $R_c$  is slightly larger than  $R_0$  in almost all determinations;  $R_c/R_0$  is situated in the interval 1.02 to 1.14, the best estimate being  $R_c/R_0 = 1.08 \pm 0.08$ .  $R_c$  is roughly proportional to the adopted value of  $R_0$ , and depends very little on  $V_0$ . Within the precision of our method and the limitations of our sample, the three main arms seen in the solar neighborhood present the same rotation velocity. Our results strongly favor the idea that the spiral pattern rotates like a rigid body. The pattern rotation speed is 25  $\text{km s}^{-1} \text{kpc}^{-1}$ , which situates the ILR and OLR at 2.5 and 12 kpc, respectively, for  $R_0 = 7.5$  kpc and  $V_0 = 190 \text{ km s}^{-1}$ . Considering that the Galaxy has an important 4-arms mode, the corresponding ILR and OLR ( $\Omega \pm \kappa/4$ ) are at about 4 kpc and 10 kpc. For almost every open cluster, we can retrieve a birthplace which coincides with the position of a spiral arm at the epoch of its birth. This observation, which is not feasible in external galaxies, gives robust support to the view that spiral arms are the triggering mechanism of star formation.

The proximity of the Sun to the corotation radius means that it has a small velocity with respect to the spiral arms, and that long periods of time elapse between successive crossings of the spiral arms. The crossing of spiral arms is a probable explanation for the peaks in the history of star formation in the solar neighborhood (Rocha-Pinto et al., 2000, de la Fuente Marcos & de la Fuente Marcos, 2004). Furthermore, the encounters with spiral arms, with the larger probability of nearby supernovae explosions and of gravitational perturbation of the Oort cloud, making more objects like comets to fall towards the inner solar system, could be associated with events of mass extinction of terrestrial (or extra-terrestrial) life (Leitch & Vasisth, 1998). Finally, the corotation radius is often considered to be associated with a minimum of star formation. If the star formation rate (SFR) is related to the rate at which the interstellar gas is introduced into the arms, that can be viewed as gas-to-star transformation ma-

chines, a recipe that has been proposed is  $\text{SFR} \propto |\Omega - \Omega_p|$  (Mishurov et al., 2002). The minimum in the star formation rate close to the Sun is a condition that favors the survival of life on the Earth. Moreover, a radius with a minimum of star formation rate must correspond to a minimum of metallicity, since the enrichment of the interstellar medium in metals is related to the death of short-lived massive stars. These concepts are essential to understand the bimodal gradient of abundance of different elements in the disk (Andrievsky et al., 2004).

The work was supported in part by the Sao Paulo State agency FAPESP

#### REFERENCES

Abad, C., Vieira, K., Bongiovanni, A., Romero, L. and Vicente, B., 2003, A&A 397, 345.

Andrievsky, S.M., Luck, R. E., Martin, P. & Lépine, J. R. D., 2004, A&A 413, 159

Amaral, L.H., & Lépine, J.R.D., 1997, MNRAS, 286, 885.

Becker, W., Fenkart, R.B., 1970, IAU Symposium 38, 205

Binney, J., & Lacey, C. 1988 MNRAS 230, 597.

Binney, J. & Tremaine, S., 1987, in "Galactic Dynamics", ed. Ostriker, J. P., Princeton University Press

Bissantz N., Englmaier P., Gerhard O., 2003, MNRAS, 340, 949

Carrasco, G. & Chiosi C., 1994, A&A 288, 751-758

Carlberg, R.G., & Sellwood, J.A. 1985, ApJ 292, 79

Clemens D. P., 1985, ApJ 295, 422

de la Fuente Marcos, R., de la Fuente Marcos, C., 2004, NewA 9, Issue 6, 475

Dehnen, W., 2000, AJ 119, 800.

Dias, W. S., Lépine, J.R.D., Alessi, B. S., 2001, A&A 376, 441

Dias, W. S., Lépine, J.R.D., Alessi, B. S., 2002, A&A 388, 168

Dias, W. S., Alessi, B. S., Moitinho, A., Lépine, J.R.D., 2002, A&A 389, 871

TABLE 1  
CO-ROTATION RADIUS OBTAINED WITH DIFFERENT ROTATION CURVES.

| Curve    | Method       | $R_0$ (kpc) | $V_0$ (km/s) | $R_C$ (kpc) |
|----------|--------------|-------------|--------------|-------------|
| Flat     | circ. rot.   | 7.5         | 170          | 8.6         |
| Flat     | circ. rot.   | 7.5         | 190          | 8.1         |
| Flat     | circ. rot.   | 7.5         | 210          | 8.0         |
| Flat     | circ. rot.   | 8.5         | 190          | 9.4         |
| Flat     | circ. rot.   | 8.5         | 210          | 9.7         |
| CO based | circ rot.    | 7.5         | 170          | 7.5         |
| CO based | circ rot.    | 7.5         | 190          | 7.9         |
| Flat     | true integr. | 8.5         | 170          | 8.1         |
| Flat     | true integr. | 8.5         | 190          | 8.6         |
| CO based | true integr. | 7.5         | 170          | 8.1         |
| CO based | true integr. | 7.5         | 190          | 7.6         |

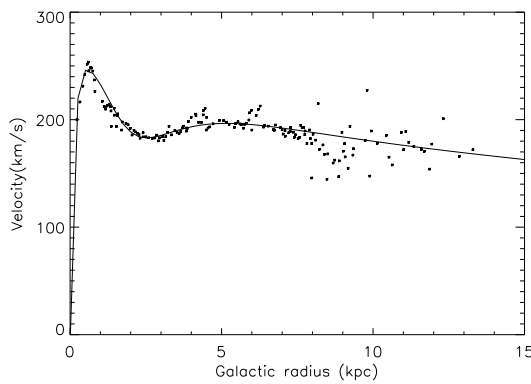


Fig. 7.— CO-based rotation curve of the Galaxy, with Clemens (1985) data corrected for  $R_0=7.5$  kpc and  $V_0 = 190$   $\text{km s}^{-1}$ . The curve is fitted by the expression  $V = 228 \exp(-r/50 - (3.6/r)^2) + 350 \exp(-r/3.25 - 0.1/r)$

Dias, W. S., Alessi, B. S., Moitinho, A., Lépine, J.R.D., 2003, EAS 10, 195

Englmaier, P., & Gerhard, O., 1999, MNRAS 304, 512.

Kalirai, J.S., et al., 2004, ApJ 601, 277

Leitch, E. M.; Vasisht, G., 1998, NewA 3, 51.

Lin, C.C., & Shu, F.H., 1964, ApJ 140, 646.

Lin, C.C., Yuan, C., & Shu, F.H., 1969, ApJ 155, 721.

Lynga, G., 1987, Computer Based Catalogue of Open Cluster Data, 5th ed., (Strasbourg; CDS)

Mermilliod, J. C., 1995, in Information and On-Line Data in astronomy, ed. D. Egret & M.A. Albrecht (Dordrecht: Kluwer), 127

Mishurov, Yu.N., Lépine, J.R.D., & Acharova, I.A., 2002, ApJ Lett 571, L113.

Mishurov, Yu.N., & Zenina, I. A., 1999 a, A&A 341, 81.

Olling, R.P., and Dehnen, W., 2003, ApJ 599, 275

Roberts, W.W., 1969, ApJ 158, 123.

Racine, R.; Harris, W. E., 1993, AJ 98, 1609

Reid, M. J., 1993, ARA&A 31, 345

Rocha-Pinto, H. J., Scalo, J., Maciel, W. J., Flynn, C., 2000, ApJ 531, L115

Seiden, P. E. & Gerola, H., 1979, ApJ 233, 56.

Sellwood, J.A., & Carlberg, R.G., 1984, ApJ 282, 61.

Shu, F.H., Million, V., Gebel, W., Yuan, C., Goldsmith, D.W., & Roberts, W.W., 1972, ApJ. 173, 557.

Shu, F.F., Laughlin, G., Lizano, S., & Galli, D.,  
2000, ApJ 535, 190.

Sellwood, J.A., & Binney, J.J., 2002, MNRAS 336,  
785.